

# Distributed IDM-STC versus Cooperative OFDM for the Two-Hop Decode-and-Forward Multiple-Access Relay Channel

Sebastian Vorkoeper\*, Florian Lenkeit†, Volker Kuehn\*, Dirk Wübben†, Armin Dekorsy†

\* University of Rostock, Institute of Communications Engineering  
Richard-Wagner-Str. 31, 18119 Rostock, Germany  
Email: sebastian.vorkoeper@uni-rostock.de

† University of Bremen, Dept. of Communications Engineering  
Otto-Hahn-Allee NW 1, 28359 Bremen, Germany  
Email: lenkeit@ant.uni-bremen.de

**Abstract**—This paper deals with the performance of two different access techniques for the Two-Hop Decode-and-Forward (DF) Multiple-Access Relay Channel (MARC) which includes multiple source and relay nodes. In particular, cooperative Orthogonal Frequency Division Multiplexing (cOFDM) is compared with distributed Interleave Division Multiplexing Space-Time Codes (dIDM-STC). While cOFDM requires strict synchronization in time and frequency among all communicating nodes, it allows for a rather simple detection structure. dIDM-STC, on the other hand, is very robust against timing and frequency offsets among the communicating nodes, however, requiring a more complex iterative detection. Both techniques are discussed in detail and are compared in terms of frame-error-rates (FER) and end-to-end throughput by numerical evaluations.

## I. INTRODUCTION

In recent years, research in wireless communications has not only focused on increasing peak data rates but also on decreasing the outage probability, especially for users at the cell edges. One very promising idea in order to achieve this goal is the use of relays in order to reduce path losses and introduce spacial diversity to the system. As multiple relays can be interpreted as a Virtual Antenna Array (VAA) [1], diversity exploiting techniques known from MIMO systems can also be adopted in a distributed fashion to relay systems. Depending on how the medium access is organized in the system, different techniques may be applicable.

In this paper, two fundamentally different transmit diversity exploiting strategies for the two-hop Decode-and-Forward Multiple-Access Relay Channel (MARC) are described and compared by means of numerical evaluations. On one hand, cooperative Orthogonal Frequency Division Multiplexing (cOFDM) based on orthogonal medium access via OFDMA and, on the other hand, distributed Interleave-Division-Multiplexing Space-Time Codes (dIDM-STC) [2], [3] based on non-orthogonal medium access via Interleave Division Multiple Access (IDMA) [4]. For the former, distributed Cyclic Delay Diversity (dCDD) [5] as a concrete diversity technique is considered.

This work was supported in part by the German Research Foundation (DFG) under grants KU 1221/6-1-2 and KA 841/20-2.

First comparisons of dCDD and dIDM-STC for single user systems under practical constraints as imperfect channel knowledge, timing- and carrier frequency offsets have been performed in [6]. However, recently, a Reliability-aware Iterative Detection scheme (RAID) for dIDM-STC has been proposed [7], [8], which allows to take the reliability of the detection at the relays into account for detection at the destination. It was shown, that RAID can achieve a significant performance improvement over the original detection structure [2]. Hence, in this paper, we extend and compare both schemes for the multi-user case and adopt the idea to include the relay reliabilities in order to improve the detection also for dCDD. However, since RAID requires a separate detection of all relay signals in order to perform a weighted combining at the destination, the RAID principle cannot directly be applied to dCDD, as for dCDD no separate detection at the destination is performed. Thus, we shift the weighting operation to the relays. Specifically, the decoding reliability at the relays is used in order to perform a weighting of the relays' transmit signals, effectively resulting in a weighting across all relays similar to the RAID scheme.

The remainder of this paper is structured as follows. In Sec. II the general system model is given. In Sec. III and Sec. IV cOFDM and dIDM-STC, respectively, are presented and discussed in detail. Sec. V presents numerous numerical results in terms of frame-error-rates and end-to-end throughput. Finally, Sec. VI concludes the paper.

## II. SYSTEM MODEL

We investigate the multiple-access relay channel (MARC), depicted in **Figure 1**. Multiple source nodes  $S_n$ ,  $n \in \{1 \dots N\}$  simultaneously access the channel during the first time slot  $T_1$  in order to communicate with multiple relay nodes  $R_m$ ,  $m \in \{1 \dots M\}$ ,  $M \geq N$ . All relays perform Decode-and-Forward, thus, every source message is decoded at each relay. During the second time slot  $T_2$ , the relays simultaneously forward the reencoded source information towards the destination D. Both time slots,  $T_1$  and  $T_2$ , are assumed equally long, i.e., their duration is not optimized. Furthermore,

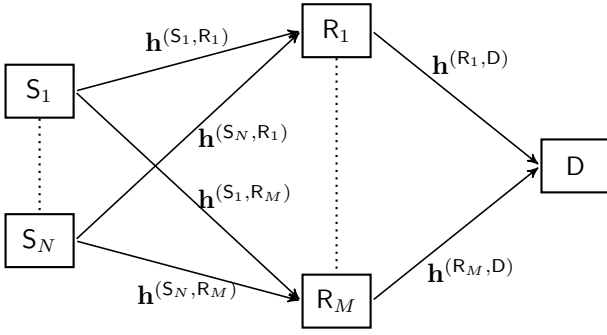


Fig. 1. Topology of the considered Two-Hop Decode-and-Forward Multiple-Access Relay Channel.

no direct links exist between the sources and the destination and it is assumed that the receivers have perfect channel state information (Rx-CSI), whereas the transmitters have no channel knowledge.

Since all source nodes transmit during  $T_1$  and all relay nodes utilize the channel during  $T_2$ , two multiple access channels are created. For the cOFDM system, the channel access by the sources during  $T_1$  is organized in an orthogonal manner using OFDMA, whereas for the dIDM-STC system the sources transmit non-orthogonally using IDMA.

In the second phase  $T_2$ , for cOFDM the relays forward the reencoded source information on the same carriers as in the first phase. Thus, the source information is also transmitted in an orthogonal manner. However, all relays simultaneously access all subcarriers, leading to a superposition of all relay signals. For dIDM-STC a distributed IDMA-Space-Time Code is applied across all relays, leading to a non-orthogonal transmission as in the first phase. Both schemes are described in detail in Sections III and IV.

The channels between any transmitting node  $t$  and any receiving node  $r$  is modeled as block Rayleigh fading frequency selective, with corresponding discrete-time channel impulse response (CIR) in vector notation  $\mathbf{h}^{(t,r)}$  containing  $L$  channel taps. Furthermore, it is assumed that the elements of the CIR are uncorrelated with average sum power

$$\mathbb{E} \left\{ \left\| \mathbf{h}^{(t,r)} \right\|^2 \right\} = \left( a^{(t,r)} \right)^2, \quad (1)$$

depending on the path loss

$$a^{(t,r)} = \sqrt{\left( d^{(t,r)} \right)^{-\alpha}}, \quad (2)$$

including the distance  $d^{(t,r)}$  between the nodes  $t$  and  $r$  and the path loss exponent  $\alpha$ . The latter is assumed to be in the range of  $2 \leq \alpha \leq 5$ , i.e., free space propagation with almost no scattering to suburban environments with strong scatterers. At each receiver  $r$ , the signal is additionally disturbed by additive white Gaussian noise  $\mathbf{n}^{(r)}$  with power spectral density  $N_0$ . Finally, all stations transmit with unit transmit power, i.e.  $\mathbb{E} \left\{ \left\| \mathbf{x}^{(t)} \right\|^2 \right\} = 1$ , where  $\mathbf{x}^{(t)}$  is the transmit signal in vector notation of node  $t$ . The receive signal in time-domain at  $R_m$  is then given as the superposition of the transmit signals of all sources convolved with the corresponding CIRs plus additive noise as

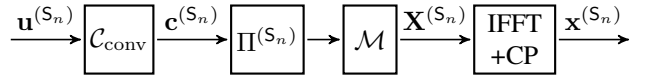


Fig. 2. Structure of OFDMA source  $S_n$  consisting of channel encoder, bit-level interleaver, symbol mapper and OFDM specific processing.

$$\mathbf{y}^{(R_m)} = \sum_{n=1}^N \mathbf{h}^{(S_n, R_m)} * \mathbf{x}^{(S_n)} + \mathbf{n}^{(R_m)}. \quad (3)$$

During the second phase  $T_2$ , the receive signal at the destination is analogous given by the superposition of the relays transmit signals  $\mathbf{x}^{(R_m)}$  convolved with the corresponding CIRs plus additive noise as

$$\mathbf{y}^{(D)} = \sum_{m=1}^M \mathbf{h}^{(R_m, D)} * \mathbf{x}^{(R_m)} + \mathbf{n}^{(D)}. \quad (4)$$

For cOFDM the frequency-domain representation of (3) and (4) is more convenient. Under the assumption of a sufficiently long Cyclic Prefix (CP), it holds

$$\mathbf{Y}_k^{(R_m)} = \sum_{n=1}^N \mathbf{H}^{(S_n, R_m)} \mathbf{X}_k^{(S_n)} + \mathbf{N}_k^{(R_m)} \quad (5)$$

and

$$\mathbf{Y}_k^{(D)} = \sum_{m=1}^M \mathbf{H}^{(R_m, D)} \mathbf{X}_k^{(R_m)} + \mathbf{N}_k^{(D)}, \quad (6)$$

where the capital letters are the Fourier transform of their lower case counterparts and  $k$  being the index of the OFDM symbol. The overall number of OFDM symbols depends on the frame length  $N_f$  and the FFT size  $N_{\text{FFT}}$ . That means, for a frame length of  $N_f$ , there exist  $1 \leq k \leq N_{\text{OFDM}}$  OFDM symbols, with  $N_{\text{OFDM}} = \lceil N_f / N_{\text{FFT}} \rceil$ . Note that in order to achieve a fair comparison among all schemes, i.e. same time and bandwidth utilization, same rate, the frame length is assumed to be always a full multiple of the FFT size.

### III. COOPERATIVE OFDM

#### A. Overview

For cooperative OFDM (cOFDM), the multiple access is organized differently in time slots  $T_1$  and  $T_2$ . During  $T_1$ , the source nodes, depicted in **Figure 2**, encode their binary information sequence  $\mathbf{u}^{(S_n)}$  with a convolutional code  $\mathcal{C}_{\text{conv}}$  in order to obtain the coded information sequence  $\mathbf{c}^{(S_n)}$ . Afterwards, the code sequence is interleaved and QPSK modulated, before each QPSK symbol is distributed exclusively among assigned subcarriers, according to the OFDMA principle. Here, as the transmitting nodes do not have channel state information (Tx-CSI), the sources have their own specific subcarriers assigned orthogonal to each other. This assignment can be random or systematic but might change per OFDM symbol in order to achieve an additional diversity gain at the relays. Neglecting the OFDM symbol index  $k$ , the frequency-domain transmit signal  $\mathbf{X}^{(S_n)}$  is transformed with the Inverse Fast Fourier Transformation (IFFT) and a Cyclic Prefix (CP) of length  $N_g$  is attached per OFDM symbol as guard interval. Thus, the resulting time-domain transmit signal is given by  $\mathbf{x}^{(S_n)}$ .

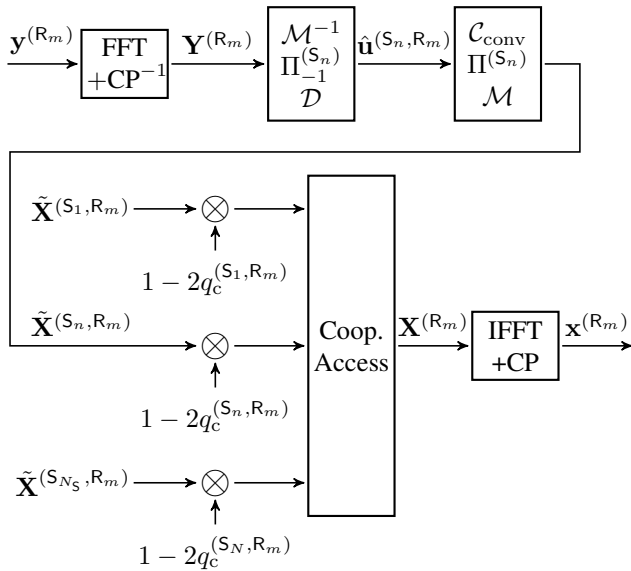


Fig. 3. Structure of OFDMA relay  $R_n$  consisting of detection chain, reencoding chain and cooperative access block.

Once the relays, depicted in **Figure 3**, receive a disturbed version  $\mathbf{y}^{(R_m)}$  of the different source signals as defined in (3),  $\mathbf{y}^{(R_m)}$  is passed through the typical OFDM receiver chain, including the removal of the CP and the FFT. Due to its orthogonal distribution among subcarriers, the coded information sequences of the source nodes are processed separately. This includes the equalization via

$$\tilde{X}_{k,\mu}^{(S_n, R_m)} = Y_{k,\mu}^{(S_n, R_m)} \cdot \left( H_{k,\mu}^{(S_n, R_m)} \right)^*, \quad (7)$$

where  $H_{k,\mu}^{(S_n, R_m)}$  is the corresponding channel coefficient for the  $k$ -th symbol on the  $\mu$ -th subcarrier. Then, demodulation  $\mathcal{M}^{-1}$ , deinterleaving  $\Pi_{-1}^{(S_n)}$  and decoding  $\mathcal{D}$  are performed. Afterwards, the hard estimates  $\hat{\mathbf{u}}^{(S_n, R_m)}$  of the binary information sequence of  $S_n$  at  $R_m$  is passed through the typical OFDM transmitter chain, which is identical to the source transmitter chain. The resulting time-domain transmit signal  $\mathbf{x}^{(R_m)}$  is then forwarded towards the destination during time slot  $T_2$ .

While the source nodes only transmit on their orthogonal assigned subcarriers the relay nodes forward all messages simultaneously, and, hence, each use all subcarriers. This is due to the fact, that all relays have an estimation of every source information and, therefore, they need to transmit on every subcarrier simultaneously, in order to forward the complete data. However, the information from different sources is still forwarded in an orthogonal manner, i.e., each subcarrier is assigned to one specific source but accessed by all relays simultaneously.

Note that the subcarrier assignment might change during subsequent OFDM symbols. Furthermore, a redistribution of messages onto subcarriers at the relays is not considered as there will be no benefits due to the Rx-CSI limitation.

In order to achieve a diversity gain, different transmit strategies across the relays are possible. In this paper, we focus on distributed Cyclic Delay Diversity (dCDD), which

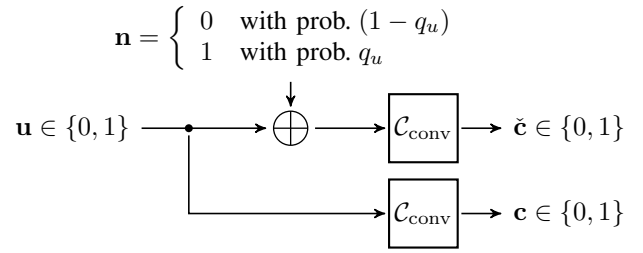


Fig. 4. Measurement setup, for calculating the dependency between  $q_u$  and  $q_c$ .

is discussed in the next section.

### B. Distributed Cyclic Delay Diversity

In case of distributed Cyclic Delay Diversity (dCDD), the relays forward a cyclically shifted version of their transmit signal  $\mathbf{x}^{(R_m)}$ . As a cyclic shift in time-domain corresponds to a phase shift in frequency-domain, the frequency-domain transmit signal in the  $k$ -th symbol on the  $\mu$ -th subcarrier  $\tilde{X}_{k,\mu}^{(S_n, R_m)}$  from (7) is processed according to

$$X_{k,\mu}^{(R_m)} = \beta_m \sum_{n=1}^N \tilde{X}_{k,\mu}^{(S_n, R_m)} \cdot e^{-\frac{j2\pi}{N_{\text{FFT}}} \mu \delta_{R_m}}. \quad (8)$$

where  $\beta_m$  is chosen in order to ensure unit transmit power for  $R_m$ . In (8),  $\delta_{R_m}$  denotes the corresponding phase shift on subcarrier  $\mu$  and OFDM symbol  $k$  for relay  $R_m$ . A cyclic shift increases the effective channel impulse response [9] [10], transforming spacial diversity offered by the relays into frequency diversity, which can be exploited by the channel code.

### C. dCDD with Reliability-aware Transmit Signal Processing

In practical systems, error-free decoding at the relays usually cannot be guaranteed. If decoding errors occur, they propagate to the destination degrading the overall performance of the system. In [7], [8] a method to estimate the decoding success and the decoding reliability of the relays in order to improve the detection at the destination was proposed. It was shown, that the resulting Reliability-aware Iterative Detection scheme (RAID) leads to a significant performance improvement compared to the original dIDM-STC detector from [2]. In order to achieve a fair comparison, we propose a method to exploit the same side information, i.e. the estimated bit error probability at the relays, also for dCDD.

The bit error rate  $q_u^{(S_n, R_m)}$  of the hard decided information sequence  $\hat{\mathbf{u}}^{(S_n, R_m)}$  for  $\mathbf{u}^{(S_n)}$  at relay  $R_m$  can be estimated via the Log-Likelihood Ratios (LLRs)  $\mathbf{L}_u^{(S_n, R_m)}$  at the decoder output [11] as

$$q_u^{(S_n, R_m)} = \mathbb{E} \left\{ \frac{1}{1 + e^{\mathbf{L}_u^{(S_n, R_m)}}} \right\} \approx \frac{1}{N_u} \sum_{i=1}^{N_u} \frac{1}{1 + e^{L_{u,i}^{(S_n, R_m)}}}, \quad (9)$$

where  $N_u$  is the number of information bits per frame. Since for dCDD no separate detection of the relay signals is performed at the destination, we use  $q_u^{(S_n, R_m)}$  in order to perform a weighting of the relay signals before transmission to the destination. Specifically, each relay signal is weighted

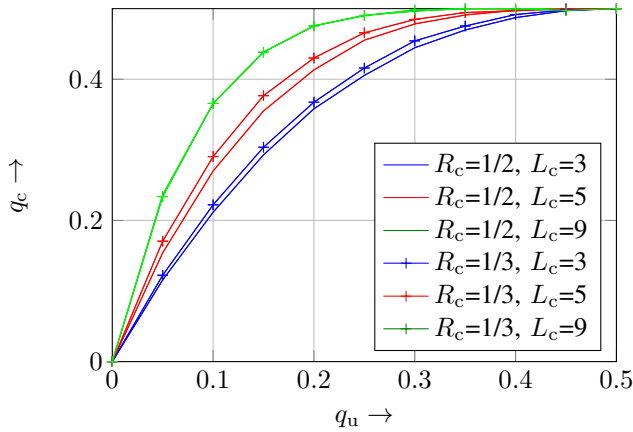


Fig. 5. Relationship between the information error rate  $q_u$  at the convolutional encoder input and the corresponding error rate  $q_c$  over the code sequence at the encoder output for codes of different rates  $R_c$  and constraint lengths  $L_c$ .

according to the error probability at the relay. However, the weighting has to be performed w.r.t to the code bit error probability and not w.r.t the information bit error probability. In order to determine the relationship between both, we use the measurement setup depicted in **Figure 4**.

Here, a randomly generated binary information sequence  $\mathbf{u}$  at the input of a convolutional encoder  $\mathcal{C}_{\text{conv}}$  of rate  $R_{c,\text{conv}}$  with constraint length  $L_c$  is altered by the modulo-2 sum with the noise sequence  $\mathbf{n}$ , which is created according to the bit error rate  $q_u$ . Afterwards, the coded information sequence  $\tilde{\mathbf{c}}$  from the altered information sequence  $\tilde{\mathbf{u}}$  is compared to the coded information  $\mathbf{c}$  from the original sequence  $\mathbf{u}$  and the error rate  $q_c$  over the code sequence is calculated.

As depicted in **Figure 5**, the bit error rates of the code sequences strongly depend on the constraint length  $L_c$ , which is quite intuitive, since one erroneous information bit may result in up to  $L_c$  erroneous code bits. This is especially true in the lower error regime, where the approximation  $q_c \approx L_c q_u$  holds, since predominantly single error events occur. Implementing the measured relationship between  $q_u$  and  $q_c$  in a lookup table, the relay signals are then weighted as

$$X_{k,\mu}^{(R_m)} = \beta_m \sum_{n=1}^N \left(1 - 2q_c^{(S_n, R_m)}\right) \tilde{X}_{k,\mu}^{(S_n, R_m)} \cdot e^{-\frac{j2\pi}{N_{\text{FFT}}} \mu \delta_{R_m}}, \quad (10)$$

where  $0 \leq q_c \leq 0.5$  is the bit error probability w.r.t  $S_n$  at  $R_m$ . For  $q_c^{(S_n, R_m)} \approx 0^1$ , the transmit signal is not altered, whereas if  $q_c^{(S_n, R_m)} = 0.5$ , the specific estimated source information is not forwarded at all, since effectively no information regarding the source information is available at the relay. After weighting the individual reencoded source messages, the overall transmit signal of each relay is scaled by  $\beta_m$  in order to achieve unit transmit power.

The benefits of this Reliability-aware Transmit Signal Processing (RATSIP) for dCDD relies in the simple receiver structure at the destination, i.e., the dCDD receiver has not

<sup>1</sup>Since the error probability is estimated using LLRs, it is always greater than zero.

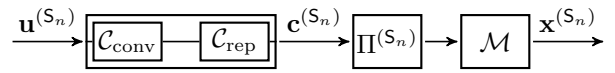


Fig. 6. IDMA source  $S_n$  consisting of channel encoder, bit-level interleaver and symbol mapper.

to be altered in order to incorporate the decoding reliabilities of the relays and, thus, conventional OFDM receivers are applicable.

#### IV. DISTRIBUTED IDM-SPACE-TIME CODING

##### A. Overview

In the first transmission phase  $T_1$ , the sources simultaneously access the channel by applying IDMA. The structure of the sources is depicted in **Figure 6**. The binary information sequence  $\mathbf{u}^{(S_n)}$  of source  $S_n$  is encoded by a non-recursive convolutional code  $\mathcal{C}_{\text{conv}}$  of rate  $R_{c,\text{conv}}$  similar to cOFDM. Additionally, spectral spreading is achieved by repetition coding  $\mathcal{C}_{\text{rep}}$  of rate  $R_{c,\text{rep}}$  leading to an overall code rate of  $R_c = R_{c,\text{conv}} \cdot R_{c,\text{rep}}$ . Afterwards, the code sequence  $\mathbf{c}^{(S_n)}$  is interleaved with the source specific interleaver  $\Pi^{(S_n)}$  and QPSK modulated  $\mathcal{M}$ , resulting in the transmit sequence  $\mathbf{x}^{(S_n)}$ . Finally, all source nodes simultaneously broadcast their information towards the relays.

The structure of the relays is depicted in **Figure 7**. Each relay receives the superposition of all source signals convolved with the corresponding CIRs plus additive noise as given in (3). In order to separate the different source messages, iterative multi-user detection (MUD) based on the soft-RAKE algorithm [4] is applied. After MUD the hard decided user information  $\hat{\mathbf{u}}^{(S_n, R_m)}$  is reencoded with the same channel code  $\mathcal{C}$  as the sources and interleaved with the user specific interleaver  $\Pi^{(S_n)}$ . In order to separate the different relays at the destination, a second relay specific interleaver  $\Pi^{(R_m)}$  is applied, followed by a mapping  $\mathcal{M}$  to symbols from a QPSK alphabet. Each of the  $N \cdot M$  reencoded messages across all relays is, hereby, characterized by a unique source-relay interleaver tuple and, thus, a Space-Time Code across the  $M$  relays is formed.

At the same time, the LLRs  $L_u^{(S_n, R_m)}$  delivered by the MUD are used to estimate the bit-error-probability  $q_u^{(S_n, R_m)}$  of the information bits at the relay according to (9). Furthermore, a Cyclic Redundancy Check (CRC) is performed over the hard-decision  $\hat{\mathbf{u}}^{(S_n, R_m)}$  of  $L_u^{(S_n, R_m)}$ . In case of a correct CRC check, the relay signals an acknowledge (ACK) to the destination, while a negative CRC check leads to the signaling of a negative acknowledge (NACK) in form of the bit-error-probability  $q_u^{(S_n, R_m)}$ . Exploiting this side information, the detection performance at the destination can be increased significantly, as described in the next subsection IV-B.

In the second transmission phase  $T_2$ , the relays simultaneously broadcast their coded, interleaved and modulated sequences  $\mathbf{x}^{(S_n, R_m)}$ , with

$$\mathbf{x}^{(R_m)} = \beta_m \sum_{n=1}^N \mathbf{x}^{(S_n, R_m)} \quad (11)$$

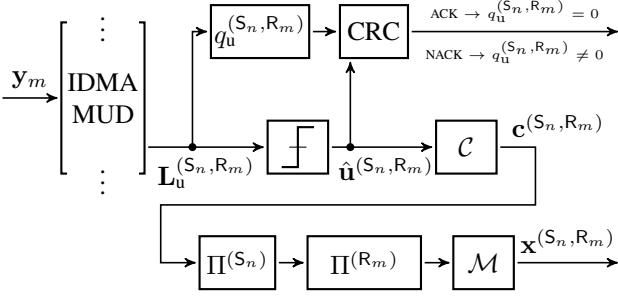


Fig. 7. IDMA relay  $R_m$  consisting of multi-user detector (MUD), error estimation chain and reencoding chain.

towards the destination. The scaling factor  $\beta_m$  hereby is chosen to ensure unit transmit power per relay. Finally, all relay signals are broadcasted simultaneously to the destination, leading to the received signal  $y^{(D)}$  according to (4).

### B. Reliability-aware Iterative Detection (RAID)

At the destination, iterative multi-user detection with respect to all  $N \cdot M$  transmitted layers is performed. Again, the soft-RAKE algorithm is used. In order to account for the different reliabilities of the relays, RAID is applied [7], [8]. **Figure 8** depicts the relevant part for detection of  $\mathbf{u}^{(S_n)}$ . Here, for illustration purposes relays  $R_1$  and  $R_2$  are assumed to be erroneous w.r.t.  $\mathbf{u}^{(S_n)}$  (upper part). Hence, they are decoded separately from all correct relays, which are decoded jointly (bottom part). After iterative detection of all relay signals, soft combining is performed, taking the different error probabilities  $q_u^{(S_n, R_m)}$  of the erroneous relays into account. Note that a detailed description of the RAID scheme can be found in [8].

## V. RESULTS

### A. System Setup

In this section, we present some results for a MARC system with  $N = 4$  sources and  $M = 4$  relays, which are placed on a two-dimensional grid at positions  $p_{S_1} = [0.0, 0.2]$ ,  $p_{S_2} = [0.0, 0.1]$ ,  $p_{S_3} = [0.0, -0.1]$  and  $p_{S_4} = [0.0, -0.2]$  for the source nodes,  $p_{R_1} = [0.5, 0.3]$ ,  $p_{R_2} = [0.5, 0.1]$ ,  $p_{R_3} = [0.5, -0.1]$  and  $p_{R_4} = [0.5, -0.3]$  for the relay nodes and  $p_D = [1.0, 0.0]$  for the destination. The number of information bits per user is fixed to  $N_b = 128$  for both systems. For cOFDM encoding with the half-rate  $[5; 7]_8$  convolutional code leads to  $N_c = 256$  code bits and after mapping to  $N_s = 128$  QPSK symbols per user. Thus, in total 512 channel uses are required to transmit all data. Hence,  $N_{\text{OFDM}} = 8$  OFDM symbols with  $N_{\text{FFT}} = 64$  subcarriers and a guard length of  $N_g = 4$  are orthogonally accessed by the source nodes, as described in Sec. III. For dIDM-STC encoding with the half-rate  $[5; 7]_8$  convolutional code and further encoding with a repetition code of rate  $R_{c,\text{rep}} = 1/4$  leads to  $N_c = 1024$  code bits and after mapping to  $N_s = 512$  QPSK symbols per user. Since all users transmit simultaneously and in the same frequency band, in total 512 channel uses are required for transmission. Note that for the results with lower rate repetition code, i.e.  $R_{c,\text{rep}} = 1/8$ ,  $R_{c,\text{rep}} = 1/16$ , the number of information bits is reduced in order to keep the number of

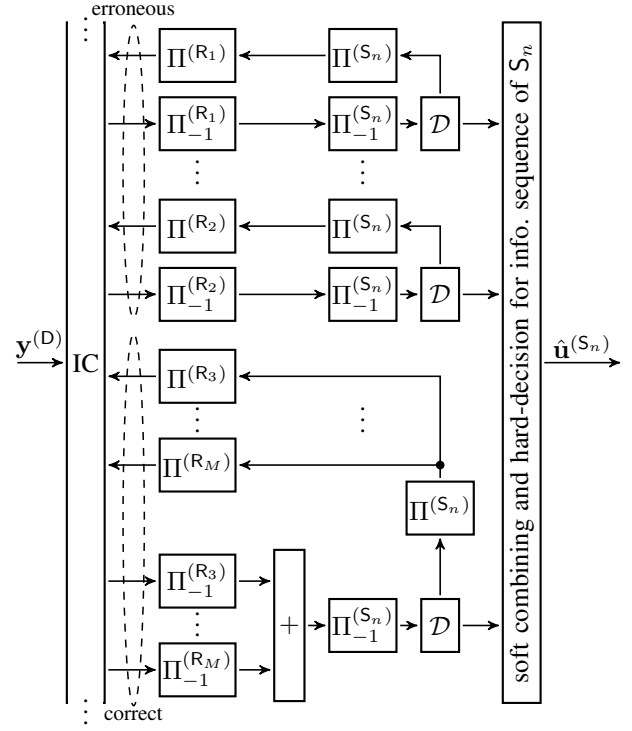


Fig. 8. Reliability-aware Iterative Detection (RAID) structure at destination D for dIDM-STC. Show is the specific part for detection of information from  $S_n$ .

required channel uses fixed. Also, in order to achieve a fair comparison, all results are given depending on  $E_b/N_0$  where  $E_b$  is the energy per information bit on the first hop. Note that the relation between the bit energy on the first and on the second hop are the same for all schemes.

### B. Flat Fading

In **Figure 9** the FERs for both schemes over flat fading channels are depicted. As can be seen, dCDD performs slightly better compared to dIDM-STC in the lower SNR region up to approx. 5 dB. The reason for this behaviour is the orthogonal transmission underlying cOFDM. While for dIDM-STC all layers are treated as interference to each other and, thus, have to be estimated and cancelled for detection, for cOFDM only the additive noise has to be coped with. Hence, conversion starts earlier for cOFDM. In order to achieve conversion for dIDM-STC for lower SNR, the code rate of the repetition code can be reduced, i.e.  $R_{c,\text{rep}} = 1/8$  or  $R_{c,\text{rep}} = 1/16$ . Due to the decoding of the repetition code during detection, which is a summation of LLRs, the noise is averaged better for the lower rate repetition codes and, hence, convergence is achieved earlier, as can be seen in the figure.

Another observation which can be made is the strongly different steepness of the FER curves of both schemes and, hence, the degree of diversity exploited by the system. While dIDM-STC exploits the full spacial diversity offered by the system, cOFDM can only achieve a diversity degree of one. The reason for this is the first hop transmission. If at least one relay is in error due to a weak first hop, dCDD severely suffers from error propagation. For comparison, the achieved

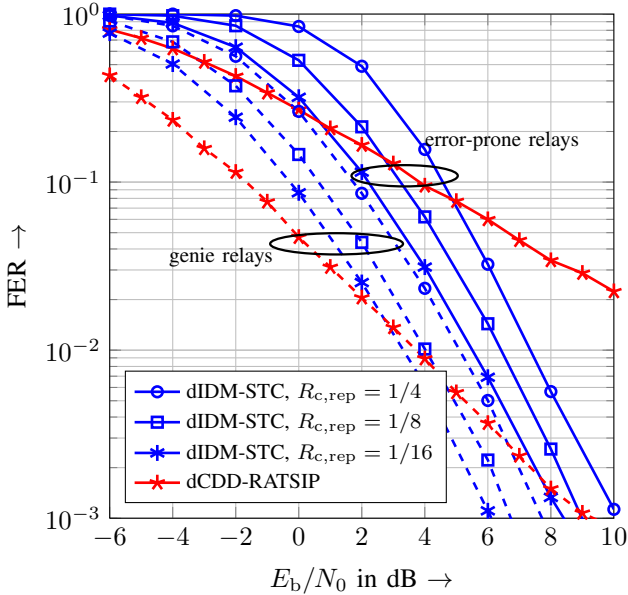


Fig. 9. FER at destination for  $L = 1$  channel tap for dIDM-STC (blue) with different repetition code rates  $R_{c,\text{rep}}$  and cOFDM with dCDD-RATSIP (red). Solid: error-prone relays; dashed: genie relays.

FERs for the same system with genie relays, i.e., perfectly decoding relays, are given (dashed). In this case, the slope of the curve for cOFDM is significantly steeper, i.e., a higher degree of diversity is exploited. For dIDM-STC in principle the overall transmission also suffers from error propagation. But since RAID is applied at the destination, effectively only the correct relays are exploited in full for detection, while the erroneous relays deliver side information depending on their reliability [8]. Therefore, dIDM-STC achieves full diversity and for genie relays, no further diversity gain, but only an SNR gain can be observed.

Under assumption of a selective repeat ARQ protocol, the end-to-end throughput of the system is given as

$$\eta = N \cdot \log_2(|\mathcal{A}|) \cdot R_c \cdot (1 - \text{FER}), \quad (12)$$

where  $N = 4$  is the number of users,  $|\mathcal{A}| = 4$  is the cardinality of the modulation alphabet and  $R_c$  is the total code rate. **Figure 10** depicts the end-to-end throughput  $\eta$ . Up to approx. 5 dB both dCDD achieves a higher throughput than dIDM-STC. Above 5 dB dIDM-STC quickly converges to the maximum throughput of 1 bits/s/Hz while convergence for cOFDM is slower. The maximum possible throughput of both dIDM-STC variants with lower code rate is limited to 0.5 bits/s/Hz and 0.25 bits/s/Hz, respectively. Note that the throughput highly depends on the code rate  $R_c$  in the system.

### C. Frequency-Selective Fading

The channel is now assumed to be frequency-selective with  $L = 4$  channel taps. The FERs are depicted in **Figure 11**. For dIDM-STC and  $R_{c,\text{rep}} = 1/4$  now an error floor can be observed. This is due to soft-RAKE detection which requires all layers and multi-path propagations to be resolved separately, such that in total  $N \cdot M \cdot L = 64$  layers have to be resolved. By defining the load of the system in terms of layers

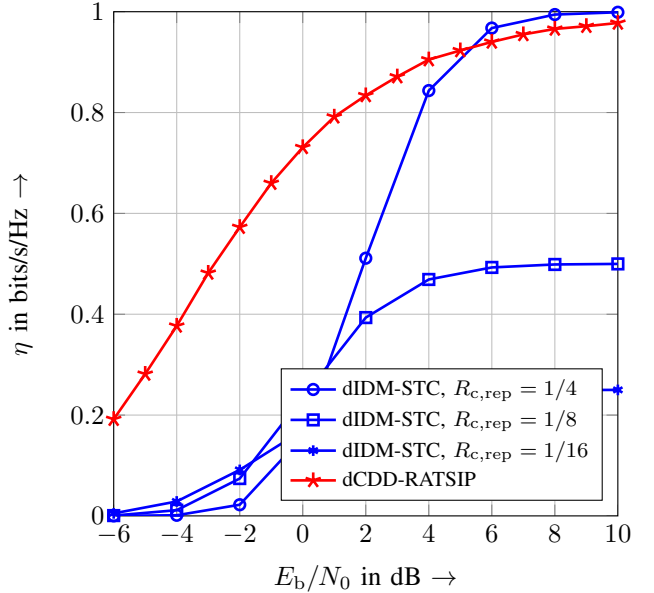


Fig. 10. End-to-end throughput at destination for  $L = 1$  channel tap for dIDM-STC (blue) with different repetition code rates  $R_{c,\text{rep}}$  and cOFDM with dCDD-RATSIP (red).

similar to [8], this corresponds to a load on the second hop of  $\beta = N \cdot M \cdot L \cdot R_c = 8$ , which is clearly too high to achieve conversion. Reducing the code rate of the repetition code to  $R_{c,\text{rep}} = 1/8$  or  $R_{c,\text{rep}} = 1/16$  and the corresponding load to  $\beta = 4$  or  $\beta = 2$ , again achieves conversion for the Multi-User Detection. The principle relations between cOFDM and dIDM-STC are the same as for the flat fading case. For a sufficiently low code rate dIDM-STC with RAID achieves full diversity, while cOFDM suffers from error propagation from the relays.

In **Figure 12** the corresponding throughput is shown. Clearly, dIDM-STC does not reach the maximum throughput anymore due to the error floor.

### D. Performance gain through RATSIP

While the significant performance gain due to RAID for dIDM-STC has been thoroughly discussed in [8], in **Figure 13** some performance comparisons for RATSIP are given. Depicted are the FERs for dCDD with and without RATSIP for two different code constraint lengths. As can be seen, for the weaker code ( $L_c = 3$ , solid) RATSIP achieves a small performance gain compared to conventional dCDD. By applying a stronger code ( $L_c = 9$ , dashed), the performance improvement with RATSIP is increased leading to a gain of approx. 1 dB at an FER of  $10^{-2}$ .

## VI. CONCLUSION

In this paper, the performance of two fundamentally different transmit diversity techniques for the Decode-and-Forward (DF) Multiple-Access Relay Channel (MARC) were compared, namely distributed Cyclic Delay Diversity (dCDD) based on orthogonal medium access via OFDMA and distributed Interleave-Division-Multiplexing Space-Time Coding (dIDM-STC) based on non-orthogonal medium access via

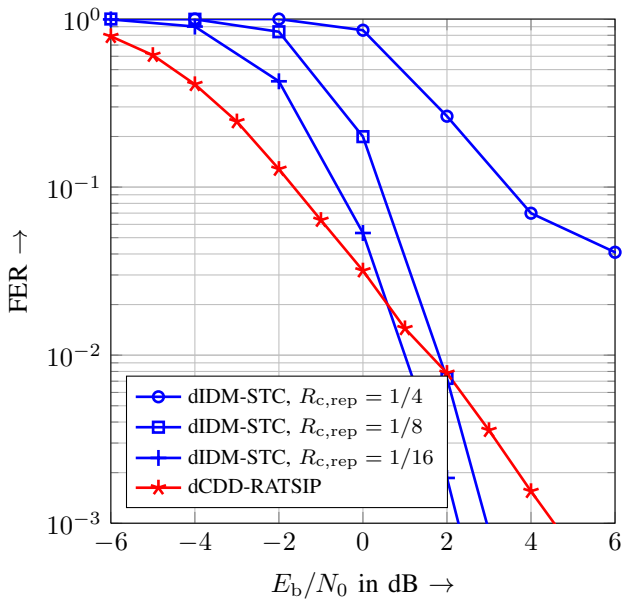


Fig. 11. FER at destination for  $L = 4$  channel taps for dIDM-STC (blue) with different repetition code rates  $R_{c,rep}$  and cOFDM with dCDD-RATSIP (red).

IDMA. In order to cope with decoding errors at the relays, the bit-error-probability at the relays was estimated and used as side-information for both schemes. As could be seen by means of numerical evaluations, dIDM-STC always exploits the full diversity offered by the system, for flat as well as for frequency-selective channels, while dCDD severely suffers from error propagation at the relays. However, due to the orthogonal medium access, no interference has to be coped with for dCDD and, thus, convergence can be achieved for lower SNRs as for dIDM-STC. This has direct impact on the end-to-end throughput in the system, which reaches its maximum for lower SNRs compared to dIDM-STC.

## REFERENCES

- [1] M. Dohler, *Virtual Antenna Arrays*, Ph.D. thesis, King's College London, 2003.
- [2] W.K. Leung, K.Y. Wu, and Li Ping, "Interleave-Division-Multiplexing Space-Time Codes," *IEEE Vehicular Technology Conference (VTC-Spring 2003)*, vol. 2, pp. 1094–1098, Oct. 2003.
- [3] Z. Fang, L. Li, and Z. Wang, "An Interleaver-Based Asynchronous Cooperative Diversity Scheme for Wireless Relay Networks," in *IEEE International Conference on Communications*, Beijing, China, May 2008.
- [4] L. Ping, L. Liu, K.Y. Wu, and W.K. Leung, "Interleave-Division Multiple-Access," *IEEE Transactions on Wireless Communications*, vol. 5, no. 4, pp. 938–947, Apr. 2006.
- [5] S. Ben Slimane and A. Osseiran, "Relay Communication with Delay Diversity for Future Communication Systems," in *Proc. VTC-2006 Fall Vehicular Technology Conf. 2006 IEEE 64th*, 2006, pp. 1–5.
- [6] S. Vorköper, F. Lenkeit, D. Wübben, V. Kühn, and A. Dekorsy, "Performance Comparison of Distributed IDM-STC versus Cooperative OFDM for practical Decode-and-Forward Relay-Networks," in *International ITG Workshop on Smart Antennas (WSA'12)*, Dresden, Germany, March 2012.
- [7] F. Lenkeit, D. Wübben, and A. Dekorsy, "An Improved Detection Scheme for Distributed IDM-STCs in Relay-Systems," in *IEEE 76th Vehicular Technology Conference (VTC2012-Fall)*, Québec, Canada, Sep 2012.

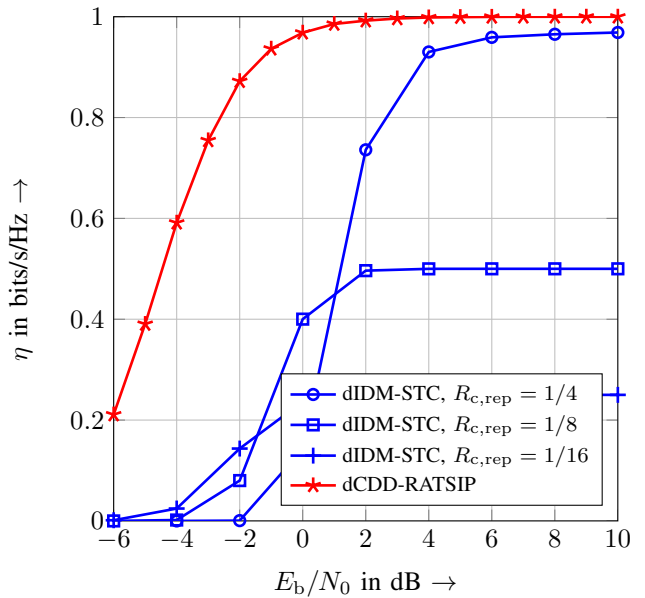


Fig. 12. End-to-end throughput at destination for  $L = 4$  channel taps for dIDM-STC (blue) with different repetition code rates  $R_{c,rep}$  and cOFDM with dCDD-RATSIP (red).

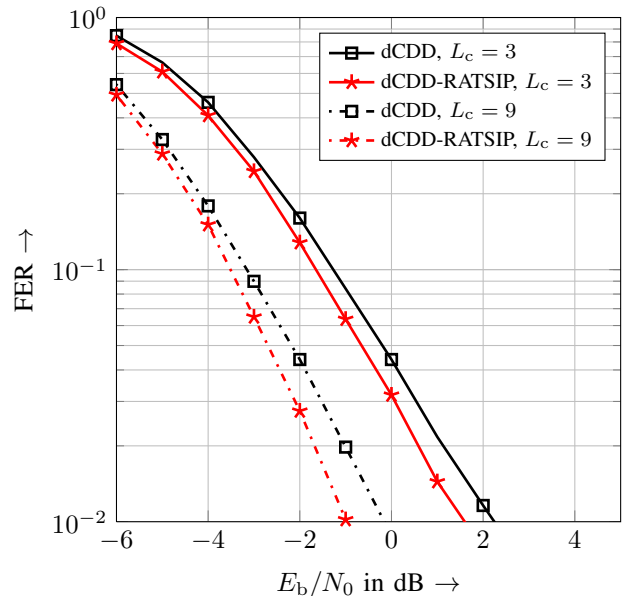


Fig. 13. Performance comparison for dCDD-RATSIP for different code constraint lengths  $L_c$  and  $L = 4$  channel taps.

- [8] F. Lenkeit, D. Wübben, and A. Dekorsy, "Reliability-Aware Iterative Detection Scheme (RAID) for Distributed IDM Space-Time Codes in Relay Systems," *EURASIP Journal on Advances in Signal Processing: Special Issue on Advanced Distributed Wireless Communication Techniques - Theory and Practice*, 2013.
- [9] I. Gaspard and J. Winter, "A New Space Diversity Scheme for DVB-T," Tech. Rep., 5th International OFDM-Workshop (InOWo), 2000.
- [10] M. Bossert, A. Hübner, F. Schühlein, H. Haas, and E. Costa, "On Cyclic Delay Diversity in OFDM Based Transmission Schemes," Tech. Rep., 7th International OFDM Workshop (InOWo), 2002.
- [11] I. Land, *Reliability Information in Channel Decoding: Practical Aspects and Information Theoretical Bounds*, Ph.D. thesis, University of Kiel, 2005.